Cluster-Analysis Classification of Wintertime Wind Patterns in the Grand Canyon Region

PIRMIN KAUFMANN*

Cooperative Institute for Research in Environmental Sciences (CIRES), University of Colorado/NOAA Environmental Technology Laboratory, Boulder, Colorado

C. DAVID WHITEMAN

Pacific Northwest National Laboratory, Richland, Washington

(Manuscript received 5 January 1998, in final form 16 June 1998)

ABSTRACT

Twelve typical wintertime wind patterns for the Grand Canyon region were derived from a two-stage cluster analysis wind-field classification scheme. The wind measurements were collected by a surface network of 15 stations deployed for a period of approximately three months. The wind patterns are strongly influenced by the complex terrain of the region. The analyses relate the wind patterns to meteorological conditions, providing insight into the physical processes generating the wind fields. Most patterns have a distinct diurnal cycle, caused by thermally induced winds near the ground. They provide evidence that thermally forced flows are important in winter and are not easily overridden by ambient flows. Some patterns differ primarily in the ratio of high- and low-elevation site wind speeds, indicating the importance of decoupling of the low-elevation winds in this basin area from the stronger ambient winds.

1. Introduction

For air-pollution studies, it is often desirable to know how frequently specific wind patterns occur within a region. Meteorological case studies also require information on wind patterns in order to determine the representativeness of the wind fields encountered in the study period. Recognition of the existence of wind-field patterns, and their frequency of occurrence, timing, rate of evolution, and transition probabilities often prove useful in gaining understanding of the physical processes or mechanisms producing the wind-field patterns.

Traditional classification schemes for weather types or wind patterns are based on meteorological experience and manual analysis of synoptic weather charts. Automated approaches that make use of cluster analysis (e.g., Mo and Ghil 1988; Bogardi et al. 1993; Cheng and Wallace 1993) have been developed as alternatives to the labor-intensive manual methods. Davis and Kalkstein (1990) and, later, Davis and Walker (1992) proposed a two-stage cluster analysis scheme to classify weather types. Weber and Kaufmann (1995) and Kaufmann and Weber (1996) applied such a scheme to the classification of wind fields from a dense network of Swiss meteorological stations in the Jura Mountains. The advantage of statistical methods like cluster analysis is that the properties of the wind-field classes need not be known in advance. In addition, the cluster analysis provides some guidance in choosing the number of classes. Although the resulting classes still depend to some extent on the choices made by the user, this method is more objective than a traditional, manual classification. The downside of an unsupervised classification is that the resulting classes are not immediately meaningful to the user and first need to be interpreted in meteorological terms.

In this paper, a two-stage cluster analysis is applied to hourly wind fields from the very complicated terrain of the Grand Canyon region of the American Southwest. A network of 15 10-m meteorological towers was operated in the Grand Canyon region of northern Arizona and southern Utah from December 1989 to beginning of April 1990 (Fig. 1 and Table 1) as part of the Navaho Generating Station Winter Visibility Study (Lindsey et al. 1999). During this study, hourly wind speed and direction were measured at each site along with other

* Current affiliation: Swiss Meteorological Institute, Zurich, Switzerland.

Corresponding author address: Dr. Pirmin Kaufmann, Swiss Meteorological Institute, P.O. Box 514, CH-8044 Zürich, Switzerland. E-mail: pka@sma.ch

© 1999 American Meteorological Society

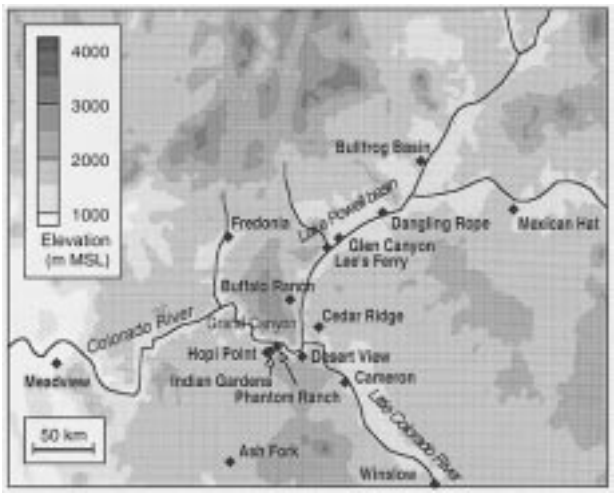

FIG. 1. Map of the Grand Canyon region showing the locations of the meteorological tower sites for the Winter Visibility Study and the National Weather Service rawinsonde station at Winslow, Arizona.

parameters. The wind vectors for the whole set of sites at a given hour are called the measured wind field or wind pattern for that hour. The wind patterns change from hour to hour but, because of the strong influence of topography, similar patterns are observed at very different times. Although the theoretical number of possible wind patterns is very large, complex topography tends to constrain the observed fields to a small number of typical patterns. The 3-month dataset used in this study allows typical wintertime flows in a region of complex topography to be described. The conclusions are restricted to one winter season. A much longer dataset (1 yr or more) would be required to determine the climatology of flows throughout the year (Weber 1998). The physical mechanisms causing the flows, however, are of a general nature and are expected to occur at other times and in other regions of complex terrain. The classification method itself is not limited to the temporal or spatial scales of this study and could be applied to a wide range of scales. The input data used here were derived from observations; however, the method could also be applied to model output data.

Wind fields in the Grand Canyon region were studied previously by Whiteman et al. (1999a) using this same dataset. Their study, however, was focused on the evolution of thermally driven winds. Specifically, they examined a subset of data for clear or partly cloudy days when synoptic-scale winds above the region were relatively weak. These ''fair weather'' conditions prevailed during only about 20% of the wintertime experimental period. In contrast, the present paper summarizes all wind patterns in the region regardless of ambient weather conditions. A comparison of Whiteman et al.'s (1999a) thermal wind patterns with the classes created by the cluster analysis provides additional insight into complex terrain flows in this region.

Section 2 provides a short review of the classification scheme and the modifications to the scheme that were made for the present study. Section 3 presents the wind field patterns found in the Grand Canyon region. The meteorological significance of the patterns is discussed further in section 4.

2. Classification method

The dataset used in this study covered the period from 19 December 1989 to 3 April 1990. At all times during this period there were valid data available from at least 8 of the 15 sites. As will be shown in this chapter, the cluster analysis used for the classification tends to be unstable if missing values are present. Therefore, a sub-

TABLE 1. Wind measurement sites and average wind speeds at the 15 sites. The averages are the scalar averages of the hourly vector averages. Column 4 is the average of a subset containing 883 h in which all sites have valid measurements. Column 5 is the average of the entire dataset from 19 December 1989 to 3 April 1990. Column 6 gives the number of valid hours used for this average, out of the 2544 possible hours.

Site name	Ident.	Elevation (m MSL)	Subset Wind speed (m s^{-1})	All data Wind speed (m s^{-1})	All data Valid hours
Ash Fork	ASH	1588	2.9	2.8	1971
Buffalo Ranch	BFL	1710	3.5	2.9	2524
Bullfrog Basin	BUL	1130	2.0	1.6	2543
Cameron	CAM	1350	2.8	2.5	2407
Cedar Ridge	CDR	1786	3.9	3.7	1793
Dangling Rope	DNG	1155	1.8	1.6	2544
Desert View	DSV	2283	3.1	2.8	2544
Fredonia	FDN	1420	2.2	2.2	2543
Glen Canyon	GCN	1314	2.9	2.7	1915
Hopi Point	HOP	2152	2.5	2.3	2277
Indian Gardens	ING	1146	1.2	1.2	1982
Lee's Ferry	LEY	994	1.6	1.4	2140
Mexican Hat	MEX	1271	1.4	1.2	2538
Meadview	MVW	1070	3.2	2.8	2520
Phantom Ranch	PTN	750	1.3	1.3	1633

set of this dataset containing about one-third or 883 of the total of 2544 available hours was used to derive the classes. The reduced dataset covered the period from 20 January to 19 March 1990, when all the stations were installed and operating.

In order for any clustering scheme to work properly, a measure of dissimilarity or distance between wind patterns is required. The distance measure of Weber and Kaufmann (1995) and Kaufmann and Weber (1996) is used with a slight modification. The stations in the present study exhibited a wide range of average wind speeds (Table 1). To prevent the stations with generally high speeds from getting an overweighting in the distance measure [to be defined later in Eq. (5)], the wind components u_{ij} and v_{ij} at each time i and station j were normalized by dividing by the time-average speed s_j at each site to obtain

$$u'_{ij} = \frac{u_{ij}}{s_j}, \qquad v'_{ij} = \frac{v_{ij}}{s_j}, \tag{1}$$

where

$$s_j = \frac{1}{M_j} \sum_{i=1}^{M_j} (u_{ij}^2 + v_{ij}^2)^{1/2}, \tag{2}$$

and M_j is the total number of hourly winds at the site.

The normalization according to Eqs. (1) and (2) was not used by Weber and Kaufmann (1995). This is the mentioned slight difference between their distance measure and the one used here.

After normalization of the hourly wind measurements at each of the sites, the individual wind patterns were normalized. The wind components u'_{ij} and v'_{ij} are divided by the spatial-average speed s'_i at each time i to obtain

$$\tilde{u}_{ij} = \frac{u'_{ij}}{s'_i}, \qquad \tilde{v}_{ij} = \frac{v'_{ij}}{s'_i}, \tag{3}$$

where

$$s'_i = \frac{1}{N_i} \sum_{j=1}^{Ni} (u'^2_{ij} + v'^2_{ij})^{1/2}, \tag{4}$$

and N_i is the total number of sites at time i.

The normalization according to Eqs. (3) and (4) ensures that similar flow patterns, which differ only by an overall scaling factor, are grouped into the same class (Weber and Kaufmann 1995). The results presented in the following sections will demonstrate that the method still picks up speed differences and builds classes according to relative speed differences within the wind fields.

The distance between two wind patterns at arbitrary times a and b was defined by

$$d_{ab} = \frac{1}{N_{ab}} \sum_{j=1}^{N_{ab}} [(\tilde{u}_{aj} - \tilde{u}_{bj})^2 + (\tilde{v}_{aj} - \tilde{v}_{bj})^2]^{1/2}, \tag{5}$$

where N_{ab} is the total number of sites that are available at both times a and b.

The purpose of a classification is to break a large number of discrete hourly wind-field patterns down into discrete classes of patterns. Ideally, all wind-field patterns within a class exhibit close similarities, while patterns in different classes are significantly different.

A two-step classification scheme for weather patterns was proposed by Davis and Walker (1992). They used a hierarchical cluster analysis to find initial clusters, which are then used as seeds for a nonhierarchical clustering method. Kaufmann and Weber (1996) adapted this suggestion for use with hourly wind fields. They used a different hierarchical method for the first step, namely, the complete linkage method, and a variant of the nonhierarchical k-means method for the second step. They retained the dissimilarity measure for hourly mesoscale wind patterns proposed by Weber and Kaufmann (1995). The two-stage classification scheme used in this study closely follows the method proposed by Kaufmann and Weber (1996). The only change from their method is the additional normalization as described by Eqs. (1) and (2).

Ideally, the outcome of a cluster analysis would not depend on the actual method used, because each method should find the same groups that exist in the data. In practice, the grouping of the data is not always clear, and certain methods may yield more useful groups than others. Weber and Kaufmann (1995) found the complete linkage clustering method to be best suited for the classification of wind patterns. The complete linkage algorithm is invariant under monotone transformations of the distance measure (Jain and Dubes 1988). Thus, the result of the cluster analysis does not depend on whether the dissimilarity [Eq. (5)] or, for example, the square of that quantity is used. This method also has a tendency to build equal-sized clusters, whereas others either tend to build one huge cluster and many tiny ones, or build near-equally sized clusters under all circumstances (Weber and Kaufmann 1995). For a comprehensive description of cluster analysis and the properties of the numerous methods we refer the reader to Jain and Dubes (1988) or Anderberg (1973).

A simple method was used for determining the number of classes. A hierarchical cluster analysis like the complete-linkage method consists of a series of mergers, starting from initial clusters of which each contains one hourly wind pattern and ending with one cluster containing all hours. Both the beginning and end of the clustering sequence are undesirable classifications, and the task is to stop the merging of clusters at a reasonable number. Figure 2 provides the sequence of dissimilarities for each step for which two clusters are merged into one. For the complete linkage algorithm, this quantity is the maximum dissimilarity within the newly built cluster. If a relatively large jump occurs in the sequence, this indicates that two very unequal clusters have been merged into one. The clustering sequence is best stopped before such a merger occurs. In our study, the result of the complete linkage clustering stage indicated that 6,

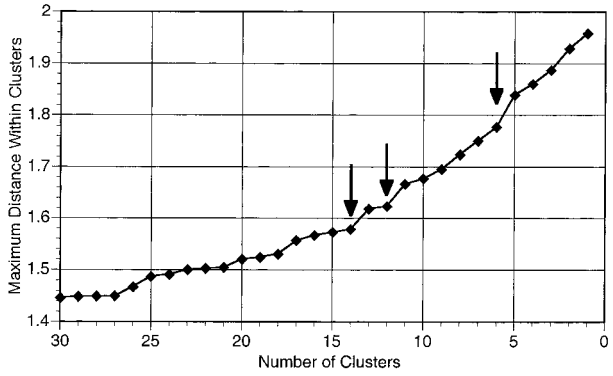

FIG. 2. Sequence of dissimilarities at which clusters merge (maximum dissimilarity within newly built cluster). The cluster analysis proceeds from left to right. The arrows indicate preferred choices for the numbers of clusters at which to stop the clustering algorithm.

12, or 14 (indicated by arrows in Fig. 2) are appropriate numbers of classes. Six classes were insufficient, in our opinion, to represent the range of meteorological conditions, and the 14-classes solution divided two classes into four newer classes with details that we did not consider important. Thus, the 12-class solution was chosen as a practical result. However, it is important to understand that the result at a lower number of clusters is achieved by merging the clusters that existed at a higher number of clusters, so that results of the cluster analysis with different numbers of clusters are closely related.

A cluster analysis is considered stable if small changes in the primary data produce only slightly different clustering results. The stability of the complete linkage algorithm was tested with two preliminary datasets, differing only by the substitution of one single hourly wind field. The result was disappointing in that most clusters in one analysis were split into two or more clusters in the other analysis. The contingency table (Table 2) clearly shows this splitting. The splitting of wind fields into other clusters was not random but, rather, involved a shifting between cluster boundaries. Experiments with other partially changed datasets revealed that the presented case is actually an extreme case of cluster rearrangement. The substituted wind field provoking the large change in the clustering solution contained missing values at a unique (i.e., nonredundant) and important measurement site, namely, Cedar Ridge (see Table 1 or Fig. 1). This site is important because, as will be shown in section 4, some flow patterns are mainly distinguished by the wind direction at Cedar Ridge. With only 15 stations, missing values at an important station can turn the wind field into an outlier that significantly disturbs the cluster analysis. Two other hierarchical methods that were described by Weber and Kaufmann (1995) as sharing the tendency to build equal-sized clusters (their Table 1), the average-distance-within-clusters method and the Ward's method, showed similar instability of the results. We concluded that a change in the clustering method did not remedy the problem and that the only way to avoid the observed instability was to avoid missing values that disturb the cluster analysis.

The effect of outliers is to extend the cluster boundary in one direction away from its mathematical center. In a hierarchical cluster analysis, the outlier remains with a cluster once it is assigned to it and cannot change to a more appropriate cluster during the analysis. In contrast, a nonhierarchical method like the k-means method allows the elements to change to another cluster. This allows the cluster boundary to realign around the mathematical center of the cluster. The drawback of the k-means method is that the number of clusters must be given in advance and that it requires initial cluster centers as seed values. The solution is to combine the two methods into a two-step classification. The hierarchical complete linkage as a first step produces initial clusters which are then, in a second step, realigned by the nonhierarchical k-means method.

We used a variant of the k-means method similar to Wishard's variant (Anderberg 1973) as a second step as proposed by Kaufmann and Weber (1996). This variant uses a threshold value d_{limit} of the distance measure. If a wind pattern has a dissimilarity greater than this

TABLE 2. Contingency table comparing the results of the complete linkage cluster analysis (first stage of the classification scheme) for two slightly different test datasets. The rows are the resulting wind-field classes using the dataset that includes the destabilizing outlier wind field. The columns are the resulting wind classes when the destabilizing outlier wind field is omitted. The main diagonal contains the number of hours for which the results coincide. These are only 41% of the total number of hours and 65% of the hours in classes 1 to 10.

Cluster	1	2	3	4	5	6	7	8	9	10	11	12
1	248	0	0	0	13	0	13	0	0	0	0	27
2	15	208	0	3	5	0	0	0	7	0	3	14
3	0	0	181	42	0	0	0	0	0	0	0	0
4	0	103	0	170	0	0	11	0	9	0	34	0
5	0	9	0	23	128	0	71	0	0	0	0	2
6	0	0	0	0	0	55	0	0	0	14	0	0
7	0	0	66	0	0	0	34	0	0	0	0	0
8	0	0	0	63	0	0	0	30	0	8	0	0
9	0	0	0	0	5	0	0	0	26	0	0	4
10	132	0	0	0	0	0	0	0	8	22	2	0
11	0	0	0	0	0	54	0	23	0	0	0	0
12	0	0	0	25	0	0	0	0	9	0	0	0

TABLE 3. Contingency table comparing the results of the k-means cluster analysis (second stage of the classification scheme), using the clusters of Table 2 as seeds. Column X and row X represent the unclassifiable patterns. A higher portion of the hours are now on the main diagonal. The k-means step could not make the completely different clusters 11 and 12 from Table 2 coincide. The main diagonal now contains 53% of all hours and 87% of the hours in classes 1 to 10.

Cluster	1	2	3	4	5	6	7	8	9	10	11	12	X
1	222	0	27	3	1	0	0	3	0	0	0	0	2
2	0	136	0	0	0	0	0	0	0	0	0	52	1
3	0	0	149	0	0	0	0	23	0	0	0	25	4
4	0	6	0	78	0	0	0	0	0	0	44	0	3
5	0	0	0	2	85	0	0	0	0	0	30	0	1
6	0	3	0	1	0	90	0	0	0	0	0	63	9
7	10	0	0	0	0	0	89	0	0	0	0	0	0
8	3	1	1	16	0	0	0	70	0	0	0	1	2
9	0	0	0	0	0	0	0	0	33	0	0	0	7
10	0	0	0	0	0	0	0	0	39	14	0	0	1
11	0	0	0	0	0	4	0	0	0	0	8	0	55
12	2	0	27	0	0	0	4	1	0	4	0	0	18
X	2	1	7	2	13	30	1	1	3	3	7	9	367

threshold value to all the cluster averages, it is considered an outlier and is not used to calculate the new cluster centroids for the next iteration step. All outliers are collected into a special group, called the outlier wind fields or the unclassifiable wind fields. Both steps of the classification, the complete linkage and the k-means cluster analyses, used the same distance measure [Eq. (5)].

Ideally, the threshold value should be sized so that each individual wind pattern is within this distance of only one cluster center. If the threshold value is too small, many patterns will be outliers, fitting into none of the clusters. If the threshold value is too large, many patterns will be within this distance of more than one cluster center and will not be recognized as outliers even if their distance is large to all cluster centers. For our purposes, the threshold value d_{limit} was chosen to be 0.8 by examining the frequency distribution of the distances between the wind fields and the cluster centers and choosing a local minimum.

We found that using a two-step procedure can significantly improve the stability of the cluster analysis. The improvement in stability for the extremely unstable case described above is considerable for the larger clusters, as seen in Table 3. For classes 1–10, fewer cases are moved off the main diagonal after the k-means analysis. Cases in the two smallest classes (11 and 12) were, however, reclassified by the k-means analysis, just as they were by the complete linkage step.

Because the instability in the extreme case was caused by missing values, we decided to omit all hours with missing values and use the reduced dataset without missing values. This greatly increased the stability of the classification scheme. Stability tests were performed by arbitrarily omitting a small number of wind fields from the reduced dataset and comparing the results. All classifications based on major parts of the reduced dataset yielded the same classes, with only a very few hours being differently assigned.

After the classes were established using the reduced dataset with no missing values, the distances [Eq. (5)] between the class centers and all hourly wind fields of the full dataset were determined. All hours of the full dataset were then assigned to the nearest class, that is, the class to the center of which the wind field has the smallest distance. Through this reassignment, all the hours previously omitted due to missing data from one or more stations or because they were outliers (cluster X) were assigned to the most appropriate classes. All already classified hours remained in the same class, because the k-means clustering step had already assigned them to the nearest cluster center. This reassignment was made for all 2544 observed surface wind fields of the full dataset, covering the period from 19 December 1989 to 3 April 1990. Each of these wind fields had a minimum of eight valid wind measurements. The classes derived from the reassignment constitute the result of the classification and will be described in the following sections.

3. Wind-field classes of the Grand Canyon region

The 12 classes that resulted from the classification described in the previous section were sorted according to their frequency of occurrence and labeled with letters from A to L (see the appendix). Table 4 provides a short description of these 12 classes and their absolute and relative frequencies of occurrence.

Near-surface winds in complex topography usually follow a diurnal cycle. To investigate if some of the classes exhibited this periodicity, the frequency of occurrence of each class was calculated for each hour of the day (Fig. 3). Class C is the only one with a nearly constant frequency during all hours of the day. Classes A, B, E, G, J, K, and L show pronounced diurnal cycles. Of these, classes A and B occur almost exclusively during the night, classes E and G occur only during the day, J is an afternoon class, K is a morning class, and

TABLE 4. Description of the wind-field classes and their frequencies of occurrence in the period from 19 December 1989 to 3 April 1990. CDR is Cedar Ridge, DSV is the Desert View site (Fig. 1). ''Basin center'' stands for the center of the Lake Powell subbasin, located in the area between the Glen Canyon and Dangling Rope sites (Fig. 1).

Class	Number of hours	Relative frequency	Description
A	577	22.7%	Flow toward basin center, north at CDR, weak and variable at higher elevations.
B	345	13.6%	Flow toward basin center, southeast at CDR, southwest at higher elevations.
C	244	9.6%	Strong westerly winds.
D	218	8.6%	Variable winds at low elevations, northeasterly winds at higher elevations.
E	215	8.5%	Flow away from basin center, southeast at CDR, variable wind aloft.
F	187	7.4%	Northwesterly flow.
G	163	6.4%	Flow away from basin center, north at CDR.
H	159	6.3%	Southwesterly flow.
I	157	6.2%	Southwesterly flow, variable at low elevations.
J	122	4.8%	Flow away from basin center, southwesterly wind at higher elevations.
K	99	3.8%	Flow away from basin center, southeast at CDR, southwest at highest elevations only.
L	58	2.3%	Weak, variable winds.

L occurs during the day/night and night/day transition hours. The remaining classes, F, I, H, and D, show a less pronounced diurnal cycle. Classes F and I both show a preference for nighttime, whereas class H shows a preference for daytime and D for transition hours. The preferred time of occurrence for each class is listed in Table 5. Because the classification is made only for a 3-month dataset in winter, no annual cycles can be determined. However, two classes show distinct seasonal changes. Class D occurs more frequently during the beginning of the dataset and decreases toward the end. Class H, on the other hand, shows an increase in the frequency of occurrence toward the end of the dataset, that is, toward spring.

Table 5 also summarizes the meteorological properties of the classes. The solar radiation observations at Ash Fork and Cedar Ridge were used as a proxy measurement of cloudiness (Whiteman et al. 1998a). The ratio of measured daily total insolation received to the theoretical extraterrestrial insolation was calculated and stored as an index of clearness that was applied to all 24 h of that day. The average relative insolation per class is listed in column 3 of Table 5. Values greater than 64% were the first of two criteria used by Whiteman et al. (1998a) to define fair weather hours. The averages of the classes A, B, C, E, F, and G met this criterion. Classes B, D, H, I, J, K, and L had values less than 64%, indicating cloudy skies.

The field average of a wind pattern is the average speed of all sites at the specified hour. Column 4 of Table 5 provides the class average of this quantity. Average wind speeds below 1.8 m s^{-1} were considered weak (classes A, B, E, and L). All these weak wind speed classes had a pronounced diurnal cycle. Moderate speeds (greater than 1.8 m s^{-1} but less than 3.6 m s^{-1}) occurred for classes C, D, F, G, I, J, and K. Only class H had high average wind speeds (greater than 3.6 m s^{-1}).

A measure of ambient wind speed and direction (columns 5 and 6 of Table 5) were obtained from the rawinsonde winds at 70 kPa at Winslow, Arizona (location in Fig. 1). The wind components were linearly interpolated in time between the twice daily soundings to obtain hourly values. Class E is the only class with average ambient speeds less than 6.7 m s^{-1}, the second of two criteria used by Whiteman et al. (1999a) to define their fair weather hours. Low wind speeds (below 8 m s^{-1}) were found for classes A, E, and G. High wind speeds (speeds greater than 12 m s^{-1}) were found for classes H and I. All other classes (B, C, F, G, J, K, L) had moderate wind speeds (between 8 and 12 m s^{-1}).

Wind directions at 70 kPa at Winslow were from the southwest for classes H, I, and K, south to west for B and J, southwest to northwest for C, west to north for F and G, variable from south through west to north for E and L, variable from northeast through southeast to southwest for D, and, finally, variable for class A.

Pressure data (column 7 in Table 5) were derived from the geopotential height of the 70-kPa level in the Winslow soundings and linearly interpolated between soundings. High pressure (geopotential height greater than 3080 m) with a rising tendency was observed for classes A, E, G. High pressure with a falling tendency was observed for class B. Low pressure (heights below 3030 m) with a rising tendency was observed for classes C and F, while low pressure with a falling tendency was observed for classes H and I. All other classes (D, J, K, L) occurred with variable pressure.

Vertical temperature gradients (column 8 in Table 5) were determined from the temperature difference between Desert View and Cameron. The difference in altitude between these two sites is 933 m. The temperature

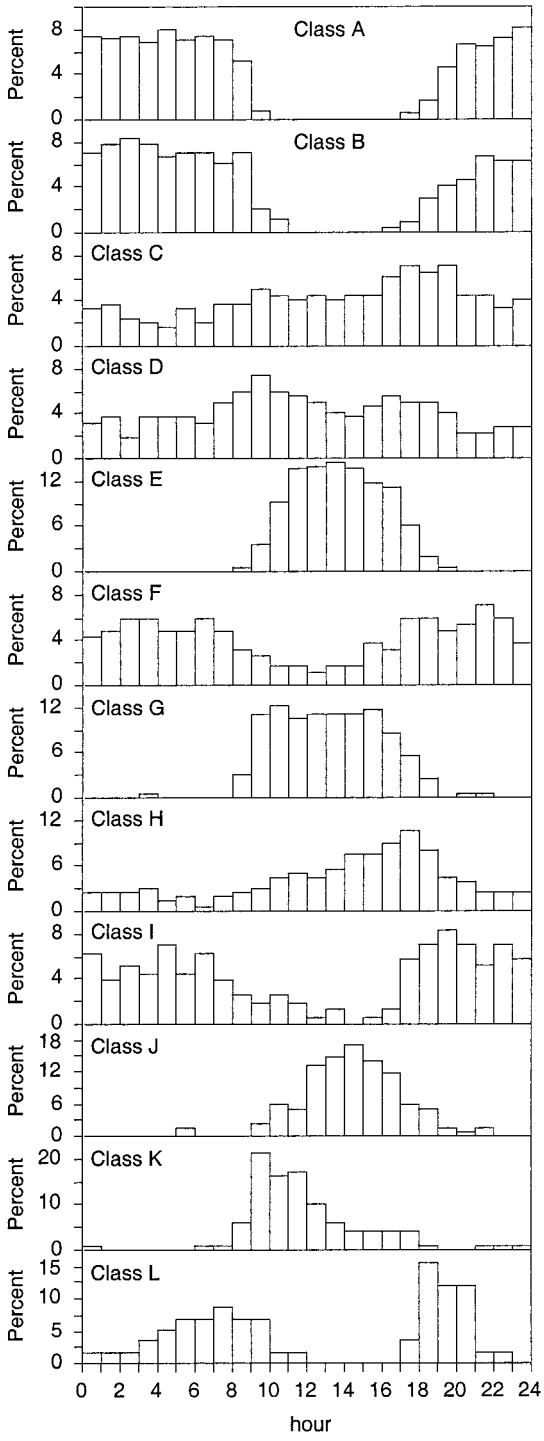

FIG. 3. Relative frequencies of occurrence of wind patterns during the different hours of the day.

gradient is defined with the z axis toward the zenith, that is, it is negative (-10 K km^{-1}) for the dry adiabatic neutral case. Although the gradient derived from these surface stations does not necessarily represent the mid-basin temperature structure well, a stable gradient is a useful indicator for the existence of an inversion in the Little Colorado subbasin. The deeper Lake Powell subbasin is even more likely to pool cold air than the Little Colorado subbasin, so we can safely assume that if a temperature inversion occurs in the latter, it is also present in the former.

The gradients were classified as very stable if the gradient was greater than -3 K km^{-1}, near neutral for gradients less than -6 K km^{-1}, and stable for values in between. Classes A, B, and K occurred with very stable conditions; classes D, E, G, and L occurred with stable conditions; and C, F, H, I, and J occurred with near-neutral stratification. By using the Cedar Ridge station, with an altitude between Desert View and Cameron (Desert View–Cedar Ridge = 497 m; Cedar Ridge–Cameron = 436 m), it was possible to determine if the gradient was more stable at altitudes above or below Cedar Ridge. The classes A, F, and mostly K show more stable stratification above Cedar Ridge, whereas I and most of J had a more stable stratification below Cedar Ridge. All other classes (B, C, D, E, G, H, and L) had near-equal stabilities (absolute difference of gradients less than 3 K km^{-1}) above and below Cedar Ridge.

The average persistence (or duration) of each class and selected transition probabilities are shown in Table 6. Class A has the highest average persistence, followed by class D. The high average persistence of class D is produced by the two periods of over 24-h duration at 17–18 and 21–22 February 1990 (see the appendix). Classes F, H, B, C, and E (in this sequence) also have high persistences. A period longer than 24 h occurs in class C on 14–16 February and in class F on 15–16 March. Between the duration of 3.8 and 3.0 h is a gap with no classes (Table 6). Classes G, I, K, and L have persistences below that gap. These are also the less frequent classes.

The highest transition probability for each class is to remain in the same class. This probability is also a measure of persistence. Table 6 lists, in addition, the highest two probabilities for a transition to other classes. The percentages in the four last columns of Table 6 are the probabilities under the condition that a transition to a different class takes place. The two nighttime classes A and B mostly change into each other (Table 6). This is an indication that the flow pattern sometimes switches back and forth during the night. The transition of A to the class D and of B to the morning class K are due to the similar winds at higher elevations within the pairs A, D and B, K. Class D then changes back to A or to the daytime class G. The morning class K is followed either by the afternoon class J or by the daytime class E. The two daytime classes E and G have the highest probabilities of mutually changing to one another. Class G is also often followed by the nighttime class A. The second highest transition probability of class E is the lowest of all percentages in Table 6 and is a transition to class C. As will be discussed later, the flow pattern of class E indicates lower surface pressure to the north,

TABLE 5. Meteorological properties of the wind-pattern classes.

Class	Time of day	Clearness index (%)	Surface wind speed	Wind speed aloft (70-kPa level)	Wind direction aloft (70-kPa level)	Pressure (70-kPa level)	Temperature gradient
A	Night	71	Low	Low	Variable	High	Very stable
B	Night	66	Low	Mod.	S–W	High, falling	Very stable
C	All day	66	Mod.	Mod.	SW–NW	Low, rising	Neutral
D	Mostly morning and evening	55	Mod.	Mod.	NE–SE–SW	Variable	Stable
E	Day	71	Low	Low	S–W–N	High	Stable
F	Mostly night	71	Mod	Mod.	W–N	Low, rising	Neutral
G	Day	75	Mod.	Low	W–N	High, rising	Stable
H	Mostly day	58	High	High	SW	Low, falling	Neutral
I	Mostly night	58	Mod.	High	SW	Low, falling	Neutral
J	Day (afternoon)	60	Mod.	Mod.	S–W	Variable	Neutral
K	Day (morning)	62	Mod.	Mod.	SW	Variable	Very stable
L	Morning and evening	64	Low	Mod.	S–W–N	Variable	Stable

and the transition to class C indicates that a front passed the area. Another class with a high transition probability to class C is class H. Here, the change in wind direction from class H to C is most probably caused by a low pressure system passing north of the area. Class J is often followed by either I or H. The latter mutually change into one another, but class I more often changes to B. Finally, the transition class L most frequently changes into one of the nighttime classes A or B.

4. Discussion of classes

The average wind pattern for each class is shown in Fig. 4. The averages were made using the actual wind fields, not the normalized patterns. The vectors in Fig. 4 are the vector averages of all hourly winds for the specified class at each site.

Classes A and B are both nighttime classes and show southwesterly flow at Buffalo Ranch, Lee's Ferry, and Glen Canyon. At Dangling Rope and Bullfrog Basin, the wind direction is northeast. Whiteman et al. (1999a) described this flow pattern as nighttime drainage flow toward the center of the Lake Powell subbasin. Although all of these sites are near the Colorado River, Buffalo Ranch, Lee's Ferry, and Glen Canyon are not directly on the river but on the platform surrounding the Marble Canyon. This platform is tilted against the flow direction of the Colorado River toward the northeast and therefore induces the southwesterly downslope winds. Thus, all five sites represent nighttime drainage flow toward the Lake Powell subbasin center.

Classes A and B show very stable temperature gradients in the Little Colorado River basin below the height of the Grand Canyon's south rim (Table 5). In class A, the average gradient is positive above Cedar Ridge and near neutral below, indicating a strong inversion just below the Canyon rim height. In class B, the layers above and below Cedar Ridge are equally stable. The strong stability in both classes is a result of the accumulation of cold air in the basin at Cameron. At Desert View, the air cooled at the ground flows to-

TABLE 6. Average persistence of classes in hours, and selected transition probabilities. The highest probability for each class is to be followed by the same class. The two highest transition probabilities under the condition that a transition to a different class occurs are listed in the four last columns.

		Transition probability				
Class	Avg. persistence (h)	To same class (%)	To class	(%)	To class	(%)
A	5.7	82	B	33	D	20
B	4.2	76	A	39	K	20
C	4.2	76	F	22	A	21
D	5.1	80	A	37	G	30
E	3.8	74	G	30	C	16
F	4.8	79	A	41	D	21
G	3.0	67	E	35	A	19
H	4.3	77	I	41	C	32
I	3.0	66	B	32	H	26
J	2.8	65	H	33	I	30
K	2.5	60	J	40	E	23
L	1.9	48	B	37	A	20

ward lower terrain and is replaced by warmer air from aloft.

Whiteman et al. (1999a), in their climatological investigation of thermally driven flows in the Grand Canyon region, used only fair weather hours (clear or partly cloudy hours for which upper winds were weak) so as to minimize the effect of ambient winds. Table 7 is provided to facilitate comparisons between these fair weather hours and the class A–L hours. It lists the fraction of fair weather hours that are contained within each of the 12 classes, as well as the relative distribution of fair weather hours in the individual classes.

Forty percent of the class A flow patterns occur during fair weather situations. Thus, the average flow pattern in class A is derived from many hours that are outside of Whiteman et al.'s (1999a) fair weather definition, but still is very similar to their 2100, 0000, 0300, and 0600 mountain standard time (MST = UTC − 7 h) patterns. A minor difference in wind direction occurs at Desert View. Whereas the fair weather patterns show variable weak winds with a southerly or westerly direction at Desert View, class A shows weak southeasterly winds at the same station. In fact, the wind at Desert View is quite variable within class A. The resulting direction is due to the southeast winds being slightly stronger within class A than winds from other directions. Class A is the most frequent pattern observed during fair weather conditions, accounting for 41% of all fair weather hours. Only 9% of the fair weather hours are grouped into class B (Table 7).

Only 15% of the hours in class B occur during fair weather periods (Table 7). The class B flow pattern differs from the class A pattern mainly at four stations: Hopi Point, Cameron, Cedar Ridge, and Desert View (Fig. 4). The most interesting difference between classes A and B is the wind direction at Cedar Ridge. Cedar Ridge shows strong northerly flow in class A, which was attributed by Whiteman et al. (1999a) to downslope flow. In class B, the average wind has a higher velocity and comes from the southeast, the upslope direction. Regarding all cases, not only fair weather cases, it seems more appropriate to describe Cedar Ridge as an indicator of interbasin airmass exchange between the Lake Powell subbasin and the Little Colorado River subbasin. In class A, with light and variable winds aloft (Table 5), air flows southeastward out of the Lake Powell subbasin into the Little Colorado River subbasin. In addition, an inversion layer above Cedar Ridge protects the site from the ambient winds. In class B, with moderate wind speeds aloft and wind directions between south and west (Table 5), the air flow at Cedar Ridge is out of the Little Colorado River subbasin and into the Lake Powell subbasin. A possible reason for the southeasterly flow at Cedar Ridge could be the horizontal pressure gradient between the subbasins. The moderate southwesterly winds aloft, if assumed to be geostrophic, indicate the existence of a pressure gradient from southeast to northwest, with higher pressure over the Little Colorado subbasin than over the Lake Powell subbasin. This pressure gradient may then force airflow near the ground from the Little Colorado subbasin to the Lake Powell subbasin.

Class C is the only class with no clear diurnal cycle (Table 5 and Fig. 3). It occurs with low pressure and neutral stratification and appears to be an advective pattern in which winds at the surface are well coupled to west winds aloft (Fig. 4). Surface winds in the Grand Canyon at the Indian Gardens and Phantom Ranch sites are turned into a more southerly or southwesterly direction by local topography, as are the winds at Lee's Ferry.

Class D occurs at all hours of the day (Fig. 3) and can therefore be considered an advective class. However, it also includes transitional patterns, because its highest frequency of occurrence is during the morning and evening transition periods. Most lower sites experience variable wind directions within this class, while the higher-elevation sites experience prevailing easterly flows. The averaging of transient and advective wind fields produces a moderate average speed for the class as reported in Table 5. The Winslow soundings show variable wind directions with this class and do not support the notion that the easterly flow might be produced by prevailing easterlies aloft. However, because this class has a higher frequency of occurrence during the beginning of the dataset, it is likely that the variable winds at lower elevations are related to a strong inversion protecting the near-surface winds from the ambient winds (Whiteman et al. 1999b). The stable gradient reported in Table 5 supports this conclusion.

Classes E and G are both daytime classes (Table 5 and Fig. 3). Most of the fair weather hours between 1000 and 1800 MST are grouped into these two classes. Both classes consist of approximately 40% fair weather cases (Table 7). The fair weather daytime wind patterns of Whiteman et al. (1999a) at 1200 and 1500 MST appear to be a mixture of classes E and G. In fact, 16% of all fair weather cases fall into class E and 11% into class G. The flow at Lee's Ferry and Glen Canyon is east and northeast, which would be down valley along the Colorado River. This direction, however, is the thermal upslope direction of the tilted Marble Platform as described by Whiteman et al. (1999a). Up-valley flow from southeast is measured at Dangling Rope and Bullfrog Basin. The flow away from the Lake Powell subbasin center at all four sites indicates daytime thermal flow.

The two classes E and G differ primarily at six stations: Fredonia, Buffalo Ranch, Desert View, Cameron, and Ash Fork. The most remarkable difference is at Cedar Ridge, where the flow comes from the southeast in class E but from the north in class G. This difference is similar to the difference found between the two nighttime classes A and B. The northerly winds in class G seem to be the result of a northerly flow aloft. Class E has flows aloft varying from southwesterly to northwesterly. This flow aloft indicates a similar pressure

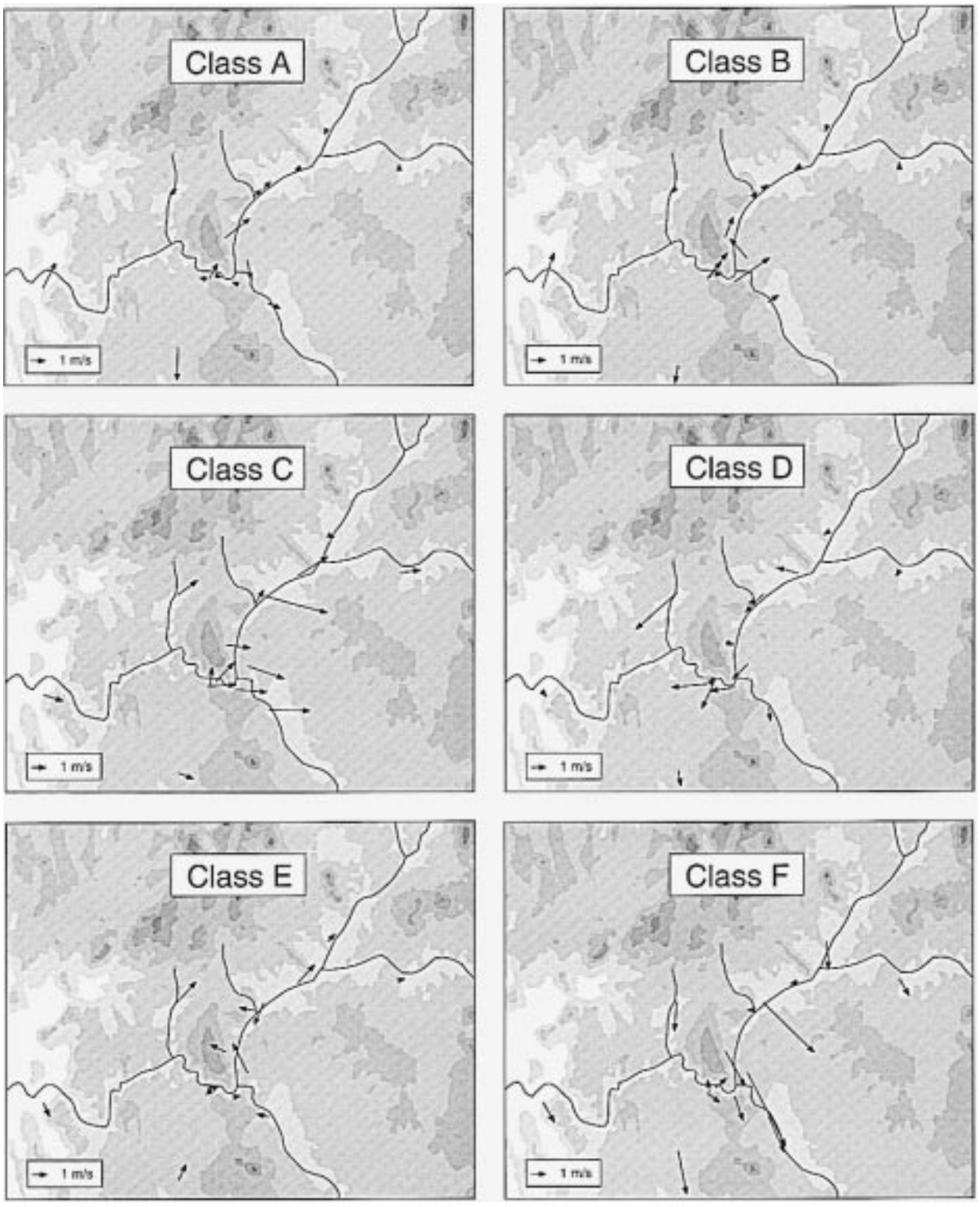

FIG. 4. Average winds for the 12 wind-pattern classes A–L.

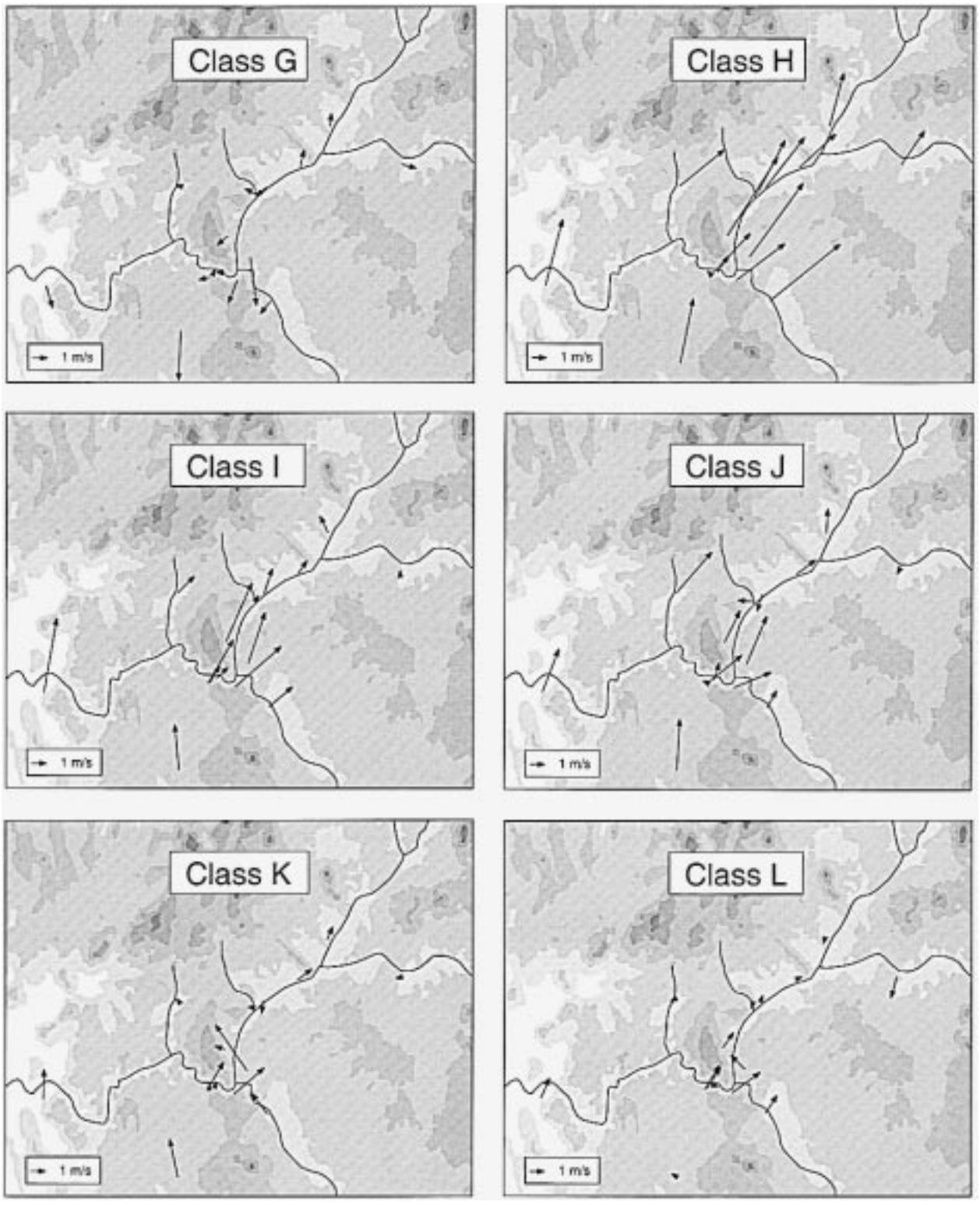

FIG. 4. (*Continued*)

TABLE 7. Comparison of hours within each class and the hours selected previously by Whiteman et al. (1999a) as fair weather cases.

Class	Number of cases		Portion (%)	
	Class total	Fair weather	Of class total	Of all fair weather cases
A	577	233	40	41
B	345	53	15	9
C	244	23	9	4
D	218	51	23	9
E	215	91	42	16
F	187	20	11	3
G	163	64	39	11
H	159	0	0	0
I	157	10	6	2
J	122	10	8	2
K	99	10	10	2
L	58	9	16	2
All classes	2544	574	23	100

pattern as for class B, resulting in flow from the Little Colorado River subbasin to the Lake Powell subbasin. Since this flow direction is also the upslope direction, it is preferred at Cedar Ridge during daytime unless there is northerly flow aloft as in class G. Both patterns occur with stable stratification (Table 5) in the Little Colorado River subbasin below the height of Desert View.

Class F has a tendency to occur at night (Table 5 and Fig. 3) and is dominated by moderate northwesterly ambient winds (Table 5). It is an advective type of flow that occurs with low but rising pressure, apparently after the passage of low-pressure systems. The average temperature gradient is neutral for the total layer between Desert View and Cameron, but stable for the layer above the Cedar Ridge height. Therefore, a weak inversion seems to be present just below the Grand Canyon south rim height.

Classes H and I occur with strong ambient southwesterly winds aloft (Table 5) and southwesterly surface winds at most sites. The time of occurrence is predominantly daytime for class H and nighttime for class I (Table 5 and Fig. 3). Both classes show neutral stratification (Table 5). It is evident from Fig. 4 that the wind speed in the Lake Powell subbasin is much higher for class H than for class I. Thus, winds in the Lake Powell subbasin seem to be better coupled to the ambient wind during daytime than during nighttime. Temperature gradient calculations for class I below the elevation of Cedar Ridge show that a shallow inversion is often present there (and presumably also in the Lake Powell subbasin) during these events. In addition, class H has a much higher frequency of occurrence toward the end of the dataset, when solar heating is stronger and an inversion in the Lake Powell subbasin is more likely to break up. Both classes occur with low pressure, and they share the lowest relative insolation of all classes. The falling pressure tendency indicates an approaching low pressure system, which fits well with the southwesterly wind direction. Whiteman et al. (1999b) showed that early in the year, the inversion in the basins is so strong that passing low pressure systems often cannot break it up. The basin inversion breaks up more readily as spring approaches. This is in accordance with our observation of an increase in the occurrence of class H later in the dataset. The diurnal cycle of both classes is not induced by thermal flow, but rather by the strength of the inversion in the subbasins that varies during the course of the day.

Classes H and I demonstrate that the classification scheme is able to separate patterns according to relative differences in wind speed. Although the absolute wind speed is lost through the normalization step in the classification, the relative speeds are retained, enabling the scheme to separate, for example, these two classes. This separation is useful because the two classes are produced by two different meteorological conditions, one featuring an inversion protecting the basin sites from the ambient wind (class I) and the other without inversion (class H).

Classes J and K are both daytime classes. Class J occurs predominantly in the afternoon, while class K occurs predominantly in the morning (Table 5 and Fig. 3). The flow within the Lake Powell subbasin is similar to that in classes E and G, representing daytime thermally driven flow. The ambient wind is southwest in both classes, but the wind at the higher stations is different. In the afternoon class J, the neutral stratification (Table 5) favors the downward transport of momentum that drives the winds at all stations except those in the Lake Powell subbasin and in the Grand Canyon, which are protected by a shallow stable layer and surrounding topography, respectively. Looking at the portion of the gradient below Cedar Ridge height, we indeed found that it was more stable than the neutral gradient above. The very stable stratification (Table 5) in the morning class K prevents the forcing of all but a few stations at the highest elevations. In fact, the gradient is more stable above Cedar Ridge than below, indicating that the inversion height is most of the time just below the Grand Canyon south rim height. The stratification is not only considerably more stable in class K than in class J, but the inversion is also at a higher altitude.

Class L (Table 5 and Fig. 3) is a transient class between daytime and nighttime flow patterns, with most sites experiencing light and variable winds. Table 5 indicates a moderate ambient wind speed and stable stratification for this class. Sixteen percent of this class are fair weather cases.

At night, thermally driven drainage flows converge toward the center of the Lake Powell subbasin. This convergence is seen in wind directions at Lee's Ferry, Glen Canyon, Dangling Rope, and Bullfrog Basin. Classes A and B are two variants of this nighttime thermal flow having differing winds at higher elevations and

accounting for 36% of all hours in the full dataset. Classes E, G, J, and K, which occur 24% of the time, represent variants of the typical daytime thermally driven flow, indicated by winds that blow away from the basin center at the above-mentioned sites. Together, the daytime and nighttime thermally driven flows occur 60% of the time within the 3-month dataset. The remaining 40% of the hourly flow patterns represent advective and transient wind cases. The clearly advective classes C, F, H, and I, with various ambient wind directions and differing influences on the low-elevation sites, constitute only 29% of the flow patterns. Class D also shows properties of an advective class, with many sites experiencing similar northwest wind directions, but the diurnal nature of class D suggests that it also contains morning and evening flow transitions that occur with northwesterly ambient wind. Class L combines the morning and evening transitions with southwesterly ambient winds.

5. Conclusions

Hourly wind fields for a 3-month period from 15 surface stations in the Grand Canyon region were classified into 12 wintertime wind-pattern classes using a two-stage cluster analysis scheme. The two-stage classification successfully improved the stability of a one-stage hierarchical cluster analysis, which was found to be sensitive to missing wind data from an important site in the region. In the present work, we eliminated all wind patterns with missing values to avoid any disturbance to the classification. After the classification, we assigned all remaining unclassified wind patterns to the most appropriate classes.

The classes were shown to be associated with differing meteorological conditions, as represented by measures of local wind speed, ambient wind, pressure, and vertical temperature gradient. The region of interest, located in the Colorado Plateau upstream from the Grand Canyon of the Colorado River, is in the form of a large basin protected by a ring of mountains and elevated mesas. Most patterns within this confined topography follow a strong diurnal cycle. However, the diurnal cycle is not always associated with thermally driven flows, as it can also be caused by the differing influences of ambient winds on the low elevation sites, as in classes H and I.

Several classes did exhibit diurnal thermally driven flows. Due to the unique pattern of these flows in the Lake Powell subbasin (Whiteman et al. 1999a), the occurrence of thermal forcing is distinguished from other forcing by the wind directions within the subbasin. Classes A and B were nighttime thermal flows, while classes E, G, J, and K were daytime thermal flows. The high frequency of occurrence of thermally driven flows, 60% of all hours in the 3-month dataset, shows that thermally driven winds are a key wintertime feature of the regional wind field. The frequency of occurrence of the thermally driven winds extends far beyond the 20% of the data contained in the small subset of clear or partly cloudy hours with weak winds aloft (fair weather hours) used in a prior study by Whiteman et al. (1999a) to investigate thermally driven winds within the region. Lower elevation sites, in particular, exhibit persistent thermally driven flows that are overridden only by strong ambient winds. The wind-field classes, while derived solely from wind data, clearly indicate the strong influence of regional and local topography. The topography causes thermally driven winds to be channeled in distinct directions at individual sites, and the cold air pool that forms within the basin often decouples the surface winds from the generally stronger winds aloft.

The present study, by dealing with all hourly wind patterns in the 3-month period, finds additional wind patterns relative to the Whiteman et al. (1999a) thermally driven wind study. Some of these additional patterns are of advective nature (classes D, F, H, I) and are not part of the focus of their study. In addition, the automated classification divided the daytime pattern into four separate groups dependent on the wind direction at Cedar Ridge and Desert View, two sites that are much more susceptible to above-basin ambient winds than are the lower-elevation sites in the Lake Powell subbasin. When winds aloft are strong, Cedar Ridge behaves more like a mountain pass site connecting the Little Colorado and Lake Powell subbasins. If strong northerly winds occur aloft during the day, the direction at Cedar Ridge blows in opposition to the thermal wind direction. The nighttime pattern is similarly divided into two groups by the classification. Here, if a strong pressure gradient is present between the two subbasins, as indicated by strong southwesterly ambient winds, the direction at Cedar Ridge opposes the drainage wind direction.

A range of ambient wind speeds occurs with thermally driven flow, which overlaps widely with the range of ambient wind speeds for advective flows. The average ambient wind speed of the advective classes C and F is moderate, as it is for the thermal classes B, G, J, and K. It is not possible to determine a critical ambient wind speed separating patterns with thermally driven winds from situations with only advective winds. The strength and height of the inversion within or above the basin is a second, important factor for the development of thermally induced flows. These findings explain why a scheme like the one used by Whiteman et al. (1999a), defining thermally driven flows by measures of ambient wind speed and radiation, considerably underestimates the actual occurrence of thermally forced winds.

The effect of passing low pressure systems depends not only on the wind speeds within the systems, but also on basin inversion strength, especially in the deepest subbasin of the area, the Lake Powell subbasin (Whiteman et al. 1999b). The classification separated two advective flow patterns with similar ambient winds but different relative speeds within the subbasin. One of them, the pattern with higher wind speeds at the low

elevation sites (class H), is more frequent during daytime and increases in frequency toward the end of the dataset, when insolation becomes stronger and the surface heating regularly breaks up the nocturnal inversion during daytime.

In summary, the flow pattern classification scheme proved to be a useful tool to gain an overview of typical wintertime flows within this complex terrain region. The length of the experimental period allowed some additional conclusions to be drawn regarding seasonal changes in wind patterns. The classes, when linked to meteorological conditions, provided insight into processes that generate the regional wind fields. Among others, the importance of the vertical temperature gradient was demonstrated for local winds. In addition, the knowledge of flow patterns is potentially useful for air pollutant studies and risk management.

Acknowledgments. Dr. Rolland K. Hauser of California State University, Chico, operated the wind network, compiled and quality controlled the datasets, and provided information on station locations and exposures. The wind data were collected as part of the Winter Visibility Study, funded by Arizona's Salt River Project (SRP), with Dr. Prem Bhardwaja as program manager. Figure 1 is based on a figure by K. J. Allwine. P. Kaufmann acknowledges support from the Paul Scherrer Institute, Switzerland. C. D. Whiteman acknowledges research support from the U.S. Department of Energy's Environmental Sciences Division (ESD) under Contract DE-AC06-76RLO 1830 at Pacific Northwest National Laboratory as part of ESD's Atmospheric Studies in Complex Terrain program. Pacific Northwest National Laboratory is operated for the DOE by Battelle Memorial Institute.

REFERENCES

Anderberg, M. R., 1973: *Cluster Analysis for Applications.* Academic Press, 359 pp.

Bogardi, I., I. Matyasovszky, A. Bardossy, and L. Duckstein, 1993: Application of a space–time stochastic model for daily precipitation using atmospheric circulation patterns. *J. Geophys. Res.*, **98,** 16 653–16 667.

Cheng, X., and J. M. Wallace, 1993: Cluster analysis of the Northern Hemisphere wintertime 500-hPa height field: Spatial patterns. *J. Atmos. Sci.,* **50,** 2674–2696.

Davis, R. E., and L. S. Kalkstein, 1990: Development of an automated spatial synoptic climatological classification. *Int. J. Climatol.,* **10,** 769–794.

——, and D. R. Walker, 1992: An upper-air synoptic climatology of the western United States. *J. Climate,* **5,** 1449–1467.

Jain, A. K., and R. C. Dubes, 1988: *Algorithms for Clustering Data.* Prentice Hall, 320 pp.

Kaufmann, P., and R. O. Weber, 1996: Classification of mesoscale wind fields in the MISTRAL field experiment. *J. Appl. Meteor.,* **35,** 1963–1979.

Lindsey, C. G., J. Chen, T. S. Dye, L. W. Richards, and D. L. Blumenthal, 1999: Meteorological processes affecting the transport of emissions from the Navajo Generating Station to Grand Canyon National Park. *J. Appl. Meteor.,* **38,** 1031–1048.

Mo, K., and M. Ghil, 1988: Cluster analysis of multiple planetary flow regimes. *J. Geophys. Res.,* **93,** 10 927–10 952.

Weber, R. O., 1998: Climatology of regional flow patterns around Basel. *Theor. Appl. Climatol.,* **59,** 13–27.

——, and P. Kaufmann, 1995: Automated classification scheme for wind fields. *J. Appl. Meteor.,* **34,** 1133–1141.

Whiteman, C. D., X. Bian, and J. L. Sutherland, 1999a: Wintertime surface wind patterns in the Colorado River Valley. *J. Appl. Meteor.,* **38,** 1118–1130.

——, ——, and S. Zhong, 1999b: Wintertime evolution of the temperature inversion in the Colorado Plateau Basin. *J. Appl. Meteor.,* **38,** 1103–1117.

APPENDIX

Hourly Wind Patterns for Winter 1989/90

	Hour of day (MST)																							
Day	0	1	2	3	4	5	6	7	8	9	10	11	12	13	14	15	16	17	18	19	20	21	22	23
Dec 19	B	B	B	A	A	A	A	A	A	C	E	E	E	E	E	E	E	C	B	B	A	A	A	A
20	B	B	A	A	A	A	A	A	A	C	C	E	E	E	E	E	E	B	B	B	A	A	A	A
21	A	A	A	A	A	A	F	F	A	G	G	G	G	E	G	G	G	A	A	A	A	A	A	A
22	A	A	A	F	A	F	A	A	A	D	G	E	G	E	E	E	E	G	A	A	A	A	A	A
23	A	A	A	A	A	A	A	A	A	D	D	G	E	E	G	G	G	F	A	A	A	A	A	A
24	A	A	A	A	D	D	D	D	D	D	D	D	D	D	G	G	D	D	D	D	D	F	D	D
25	D	D	D	D	D	D	D	D	D	D	D	D	D	D	D	D	D	D	D	D	D	D	D	A
26	A	A	A	A	A	A	A	A	A	D	D	D	D	D	D	D	D	D	D	A	A	A	A	D
27	D	D	A	A	A	A	A	D	D	D	D	D	D	G	K	D	D	B	B	B	B	B	B	B
28	B	B	B	B	B	B	B	B	B	K	K	K	J	J	J	K	K	I	B	B	B	B	A	D
29	D	D	D	D	D	D	A	D	D	D	D	D	D	D	D	F	D	F	F	D	A	A	A	A
30	A	A	A	A	A	A	A	A	A	D	G	E	G	G	G	G	G	F	F	F	F	F	D	A
31	A	A	A	A	A	A	A	A	A	D	G	E	E	E	E	E	E	E	A	A	A	A	A	A
Jan 1	A	A	B	B	A	A	B	B	B	B	K	K	K	K	J	J	J	J	B	B	B	B	I	B
2	B	B	B	B	I	I	I	I	B	I	I	J	J	J	J	C	C	C	C	E	C	F	F	F
3	F	F	F	F	F	F	F	F	F	F	F	F	C	C	C	C	E	H	C	A	A	A	F	A
4	A	A	A	A	A	A	A	D	A	G	G	G	G	E	E	E	E	E	L	A	A	A	A	A
5	F	A	A	C	F	F	F	F	C	G	G	G	G	G	G	D	G	D	F	D	F	F	A	A
6	A	A	A	A	A	A	A	A	A	A	C	E	E	E	E	E	E	C	B	B	B	B	B	B
7	B	B	B	B	B	B	B	B	B	C	C	C	E	E	E	E	E	E	E	B	B	B	B	I
8	B	A	B	B	B	B	B	C	B	C	C	C	C	E	E	E	E	C	J	C	B	B	B	B
9	B	A	B	B	A	A	A	A	A	A	G	G	E	E	E	E	E	I	B	A	A	A	A	A
10	A	B	B	B	B	B	B	B	B	B	B	E	E	E	E	E	E	L	A	A	A	A	A	A
11	A	A	A	A	A	B	A	B	B	B	B	G	E	E	G	G	G	A	A	A	A	A	A	A
12	A	A	A	A	A	B	A	A	B	B	B	K	K	K	K	K	B	B	B	B	B	B	B	B
13	B	B	B	B	B	B	B	B	B	B	B	I	J	J	H	H	H	I	I	I	B	B	I	I
14	I	I	I	I	I	I	I	I	I	I	J	E	J	J	H	H	H	H	K	C	C	J	B	B
15	L	B	I	I	I	C	I	L	L	L	J	H	J	J	J	H	H	J	I	I	I	I	I	B
16	B	B	B	B	B	B	B	A	A	K	K	K	K	J	J	J	H	I	I	I	B	B	B	B
17	I	B	B	B	L	L	L	L	D	K	D	D	D	D	D	D	D	D	D	D	D	D	D	D
18	D	D	D	D	D	D	D	D	D	D	D	D	D	D	D	D	D	D	G	F	F	F	F	F
19	F	F	F	F	F	F	F	C	C	C	C	C	J	J	J	I	C	C	C	C	C	C	C	C
20	C	C	C	F	F	F	F	F	F	F	G	D	D	G	G	G	G	G	D	D	D	D	D	D
21	D	D	A	D	A	D	D	D	D	D	D	D	D	D	D	D	D	D	D	D	D	D	D	D
22	D	D	D	D	D	D	D	D	D	D	D	D	D	D	K	K	K	L	B	B	B	B	B	A
23	A	B	B	A	B	B	A	B	L	L	L	L	J	J	J	E	J	E	J	B	G	B	B	A
24	F	F	F	F	F	F	F	F	F	F	G	G	G	G	G	G	G	G	A	A	A	A	A	A
25	A	A	A	A	A	A	B	B	B	L	K	E	E	E	E	E	E	E	L	B	B	B	B	B
26	B	B	B	B	B	B	B	B	B	K	K	K	J	J	J	J	J	H	C	C	C	F	F	F
27	F	F	F	D	D	D	D	D	D	D	D	G	G	G	G	G	G	G	A	A	A	A	A	A
28	A	A	A	A	A	C	A	A	A	A	E	E	E	E	E	E	E	E	L	L	L	B	B	B
29	B	B	B	B	B	B	B	B	L	C	H	C	C	C	C	C	C	C	C	C	C	C	B	B
30	A	A	B	B	B	B	B	B	B	K	K	K	J	J	J	J	J	I	I	I	I	I	I	I
31	I	I	I	I	I	J	K	K	L	K	K	K	K	K	J	J	J	J	J	J	L	I	I	I
Feb 1	B	B	I	I	I	I	I	I	K	I	I	I	I	I	H	J	J	J	J	J	J	J	I	C

All hours of the Grand Canyon dataset classified into 12 flow patterns. Hour 0 is the interval from 0000 to 0059 MST.

APPENDIX
(Continued)

	Hour of day (MST)																							
Day	0	1	2	3	4	5	6	7	8	9	10	11	12	13	14	15	16	17	18	19	20	21	22	23
2	C	C	F	F	F	F	F	F	F	F	F	F	F	F	F	F	F	F	F	F	F	F	F	A
3	A	A	A	A	A	A	A	A	A	A	E	E	E	E	E	E	E	K	B	B	B	B	B	B
4	B	D	B	D	D	D	D	D	D	D	D	D	D	D	D	D	D	D	D	D	F	D	A	A
5	D	D	F	F	F	F	F	F	F	G	G	G	G	C	C	J	C	C	C	C	C	B	B	B
6	A	B	B	B	B	B	B	B	B	K	K	K	K	K	K	K	K	K	L	L	B	B	B	B
7	I	B	B	B	B	B	B	B	B	K	I	J	J	J	J	H	H	H	I	I	H	C	C	C
8	C	C	C	C	C	C	C	C	C	C	C	C	C	C	C	C	C	C	C	C	A	A	A	A
9	A	A	A	A	A	A	A	A	A	G	G	G	G	G	E	E	C	E	C	C	I	C	A	C
10	B	C	B	A	A	A	A	A	A	G	G	G	G	G	G	G	G	G	F	F	A	F	F	A
11	A	A	A	A	A	A	A	A	A	G	E	E	E	E	E	G	D	D	D	D	A	A	A	B
12	B	B	B	B	B	B	B	B	B	K	K	K	K	I	J	J	I	H	H	I	I	I	I	I
13	I	I	I	I	I	I	I	I	I	H	H	H	H	H	H	H	H	H	H	H	H	H	H	H
14	H	H	H	H	H	H	C	C	C	C	C	C	C	C	C	C	C	C	C	C	C	C	C	C
15	C	C	C	C	C	C	C	C	C	C	C	C	C	C	C	C	C	C	C	C	C	C	C	C
16	C	L	L	L	L	L	L	L	K	K	K	K	K	J	J	J	J	J	I	I	I	I	I	I
17	I	H	H	H	H	H	I	H	H	H	H	H	H	H	H	H	H	H	H	H	H	H	H	H
18	I	I	I	H	I	J	I	I	H	H	H	H	H	H	H	H	H	H	H	H	I	K	K	K
19	K	F	F	L	L	L	I	A	I	L	I	I	J	H	C	C	C	C	C	C	C	C	C	C
20	C	C	A	F	F	C	F	A	C	G	G	G	C	C	C	C	C	C	H	C	A	C	A	A
21	A	A	A	A	A	A	A	A	A	G	G	G	G	G	G	F	F	F	F	F	F	F	F	A
22	A	A	A	A	A	A	A	A	A	G	G	G	G	G	G	G	E	G	F	A	A	A	A	A
23	A	A	A	A	A	A	A	A	A	G	E	E	E	G	G	G	G	G	G	A	A	A	A	A
24	A	A	A	A	A	A	A	A	A	G	G	K	E	E	E	E	E	K	A	A	A	A	A	A
25	A	A	A	A	A	A	A	A	A	B	K	K	K	E	E	E	K	K	L	B	B	B	B	A
26	A	A	A	A	A	A	A	B	A	K	K	K	E	E	E	E	E	H	A	A	A	A	A	A
27	A	A	A	A	A	A	A	A	A	B	E	E	E	E	E	G	C	F	F	F	A	A	A	A
28	A	A	A	A	A	A	A	A	A	G	G	E	E	E	D	D	G	F	D	A	A	A	A	A
Mar 1	A	A	A	A	A	A	A	A	B	K	K	K	E	E	H	E	E	E	L	A	A	A	A	A
2	A	B	B	B	B	B	B	A	B	E	K	K	K	K	J	J	J	J	L	L	L	B	B	B
3	B	B	B	B	B	B	B	B	B	E	E	K	K	J	J	J	J	J	J	L	B	B	B	B
4	B	B	B	B	B	B	B	B	K	K	K	K	J	J	J	J	J	I	I	I	I	I	I	I
5	I	I	I	I	I	I	I	H	H	H	H	H	H	H	J	H	H	H	H	H	H	C	C	C
6	C	C	C	C	C	C	C	C	C	C	C	C	C	C	C	F	C	F	F	F	F	F	F	F
7	F	F	F	F	A	A	A	A	G	G	E	E	E	E	E	E	E	E	J	I	I	B	B	B
8	B	B	B	B	B	B	B	A	A	K	E	E	E	E	E	E	E	E	L	L	L	L	L	B
9	B	B	B	B	B	B	B	B	B	K	E	E	E	J	J	J	J	I	I	B	B	I	H	I
10	B	B	B	B	B	A	B	A	B	K	J	J	J	J	H	J	I	H	I	I	I	I	I	H
11	H	H	I	I	I	H	H	H	H	H	H	H	H	H	H	H	H	H	H	H	H	H	H	H
12	H	H	H	H	I	I	B	B	I	J	J	J	J	H	H	H	H	H	H	C	C	C	C	C
13	H	C	C	C	C	C	C	C	C	C	C	C	C	F	F	F	F	F	F	F	F	F	F	F
14	F	F	F	F	A	C	F	F	G	G	C	C	C	C	C	C	F	F	C	C	F	F	F	F
15	B	F	F	F	F	F	F	F	F	F	F	F	F	F	F	F	F	F	F	F	F	F	F	F
16	F	F	F	G	A	A	A	A	G	G	G	G	G	G	G	G	G	G	G	A	A	A	A	A
17	A	A	A	A	A	A	A	A	A	E	E	E	E	E	E	E	E	E	E	A	A	A	A	A
18	A	A	A	A	A	A	A	A	G	G	G	G	G	G	G	G	G	G	G	A	A	A	A	A

APPENDIX
(Continued)

Day	Hour of day (MST)																							
	0	1	2	3	4	5	6	7	8	9	10	11	12	13	14	15	16	17	18	19	20	21	22	23
19	A	A	A	A	A	A	A	A	A	K	E	E	E	E	E	E	E	E	E	A	L	A	A	A
20	A	A	A	B	A	A	A	A	A	E	E	E	E	E	E	E	E	E	L	A	A	A	A	A
21	A	A	A	A	A	A	A	A	A	E	E	E	E	E	E	C	C	C	C	A	A	A	A	A
22	A	A	A	A	A	A	A	A	B	K	E	E	J	J	J	J	J	I	I	I	A	B	A	B
23	B	B	B	B	B	B	B	A	B	J	J	E	C	C	C	C	C	C	C	A	A	A	A	A
24	B	B	A	A	A	A	A	A	D	E	E	E	E	E	E	E	E	C	C	C	A	A	A	A
25	A	A	A	A	B	B	B	B	B	K	J	J	J	J	J	J	J	H	H	I	L	B	B	B
26	B	B	B	B	B	B	B	B	K	K	K	J	E	K	J	J	J	I	I	I	I	B	B	B
27	I	B	B	B	B	B	L	L	K	K	J	H	H	H	H	H	H	H	H	H	H	H	I	I
28	I	I	H	H	I	I	I	I	K	J	H	H	H	H	H	H	H	H	H	H	C	C	C	C
29	C	C	C	B	A	L	L	L	B	E	E	E	G	E	E	G	C	C	C	L	A	A	A	A
30	A	A	A	A	A	A	A	C	C	C	E	E	E	G	E	G	F	C	L	C	A	A	B	A
31	A	A	A	A	A	A	A	D	G	E	E	E	E	G	G	G	D	D	D	A	I	A	A	A
Apr 1	A	A	A	A	A	A	A	A	D	D	D	D	G	G	G	F	H	A	H	A	L	G	A	A
2	A	A	A	D	D	A	A	D	D	D	E	E	G	G	E	D	D	H	H	C	A	A	A	A
3	A	A	A	A	A	A	A	C	E	G	G	G	G	G	G	G	G	D	D	A	A	A	A	A